

Dynamical effects in atom optics

P. A. Ruprecht, M. J. Holland, and K. Burnett

Clarendon Laboratory, Department of Physics, University of Oxford, Parks Road, Oxford OX1 3PU, United Kingdom

(Received 11 January 1994)

We present numerical calculations of the evolution of an atomic wave packet in the optical potential created by a laser standing wave. These calculations do not rely on the Raman-Nath approximation, and fully account for transverse atomic motion within the standing wave. Our results show that atomic dynamics is important even for very brief interactions, and that the wave packet can become well localized during and shortly after the interaction. We propose several atomic beam splitters and deflectors which make use of this effect. This effect may also have repercussions for recent proposals to measure the position of an atom in a standing wave by monitoring the phase shift of the optical field; these schemes require that the field does not act back on the atom to alter its position wave function. A standing wave can also localize the wave packet in momentum space, which we show can be used to cool an atomic beam in one transverse dimension.

PACS number(s): 03.75.Be, 42.50.Vk, 32.80.-t, 32.80.Pj

I. INTRODUCTION

The deflection of an atomic beam from a laser standing wave (SW) has in recent years become a model system for investigating the interaction between atoms and an optical potential. Since a SW can diffract [1], focus [2], or split [3] an atomic beam, this configuration has been used or proposed for a variety of atom optical applications, including atom microscopy, lithography, and interferometry [4].

Much of this study, however, both experimental and theoretical, has focused on determining only the final momentum distribution acquired by the atoms as a result of the interaction. Furthermore, with a few exceptions (e.g., [5–7]), much work has been limited to approximate cases in which the interaction has close analogies to conventional (light) optics. In particular, the Raman-Nath approximation assumes that the interaction is short enough that the transverse position of the atomic wave packet remains unaltered while inside the SW. This case produces a far-field position distribution that is well described in terms of Fraunhofer diffraction of atomic matter waves from a thin phase grating [4].

We find that retaining the possibility of transverse atomic motion in a direct calculation of the atomic position and momentum distribution during and after the interaction suggests new phenomena and applications. Here, we outline a numerical study of the evolution of an atomic wave packet within an arbitrary SW potential. With it, we show that the momentum distribution predicted under the Raman-Nath approximation remains valid for interaction times far longer than those required to significantly deform the position wave function. We demonstrate atomic localization or “focusing” in the near field by propagating the wave packet through free space immediately following a brief SW interaction, and show how a subsequent interaction with a second SW can deflect or split the atomic beam. We also propose and analyze a splitting technique for pulsed beams of atoms in

which the spatial phase of the SW is shifted by a quarter wavelength partway through the interaction time. Finally, we show that a one-dimensional SW interaction can significantly compress the transverse momentum spread of an atomic beam.

II. DIPOLE FORCE AND POTENTIAL

The relevant optical force on atoms in the absence of spontaneous emission (a condition that can be met by using large detunings from resonance) is the dipole force. It arises when an atom in a laser’s electric field becomes polarized; the atom thus is subject to a force if a field gradient is present. Quantum mechanically, this force arises from momentum transfer between the atom and laser field due to photon absorption and stimulated emission cycles. In a SW composed of counterpropagating running waves, an atom that absorbs a photon from one of the running waves may be stimulated to emit the photon either back into the same wave or into the other. In the first case, the atomic momentum does not change over the cycle; in the second, it changes by $2\hbar k$, where k is the optical wave number. The direction of the dipole force can be understood most easily in the atom-field dressed-state basis. One can show [8] that in the case of negative laser detuning from the atomic resonance, the dipole force attracts ground state atoms to regions of high field intensity (SW antinodes), and for positive detuning to regions of low field intensity (SW nodes).

The dipole force is conservative, and is thus equivalent to a potential. It is straightforward to show that for detuning, $\Delta = \omega_{\text{laser}} - \omega_{\text{resonance}}$, having a magnitude much greater than the Rabi frequency, $\Omega(\mathbf{r})$, this potential has the form [9]

$$V(\mathbf{r}) = \frac{\hbar|\Omega(\mathbf{r})|^2}{\Delta}. \quad (1)$$

This optical potential is the Stark shift of a two-level atom in an oscillating field; the potential thus depends on

the strength of atom-field coupling. In a one-dimensional SW with wave number k , the Rabi frequency varies in space with the field amplitude as $\Omega(\mathbf{r}) = \Omega_0 \cos(ky)$, where Ω_0 is the Rabi frequency at a SW antinode and y is the spatial variable. Therefore the optical potential has the same spatial form as the SW intensity.

Spontaneous emissions act to destroy the spatial coherence of an atomic wave packet, and thus must be avoided in all atom optical effects that rely on interference. In this work we do not include spontaneous emission: that is, we assume that the inequality $\gamma t_{\text{int}} P_e < 1$ is satisfied. Here, γ is the natural linewidth, t_{int} is the interaction duration, and P_e is the probability that the atom is in the excited state. Note that it is possible to choose Δ and Ω_0 such that P_e , which is proportional to $|\Omega_0|^2/\Delta^2$, satisfies the inequality while maintaining the desired potential depth, $|\Omega_0|^2/\Delta$.

III. ATOMIC MOTION IN A STANDING WAVE

The scattering of an atomic beam from a SW is shown schematically in Fig. 1. The incoming atomic beam is assumed to be perpendicular to the SW and to have negligible longitudinal velocity spread. Furthermore, it is assumed to be in a minimum position-momentum uncertainty state with transverse spatial coherence greater than one standing wavelength. The atomic beam acquires transverse momentum, p_y , as a result of the interaction, and is thus deflected into one or more diffraction orders. In the “near field” immediately following the interaction, before the atomic position wave packet has evolved to match its newly acquired momentum distribution, the atoms may interact with a second SW, from which they may be further deflected. Note that laser light of a given wavelength can form a SW of an arbitrary (but greater) period if the two running waves that make up the SW are not antiparallel, but rather intersect at an angle [2].

In order to calculate the motion of a two-level atomic wave packet traversing a SW, we numerically integrate the one-dimensional Schrödinger equation in the dressed-state basis [8]. In this basis, under adiabatic conditions, an atom entering the interaction region in one dressed state will remain in that state throughout. Furthermore,

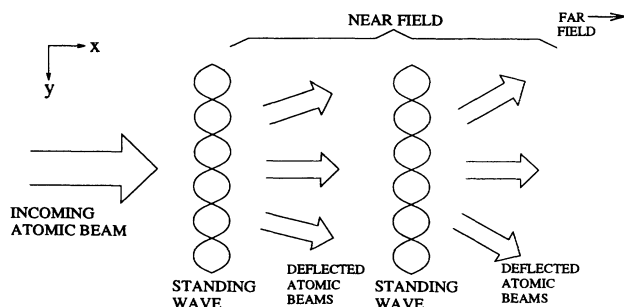


FIG. 1. Schematic for scattering an atomic beam from one or two standing waves, with coordinate axis definition.

each dressed state acts as a single-level particle moving in the optical potential given by Eq. (1). As a result, the equation which must be solved is simply

$$i\hbar \frac{\partial \phi(y)}{\partial t} = \left[\frac{-\hbar^2}{2m} \frac{\partial^2}{\partial y^2} + V(y) \right] \phi(y) \quad (2)$$

in which $\phi(y)$ is a dressed-state wave function and m is the atomic mass.

We propagate the solutions of Eq. (2) through time using the Crank-Nicolson method of numerical integration [10]. We perform the evolution in position space, and can then Fourier transform the result to obtain the corresponding momentum distribution. Since this calculation is one dimensional, the atoms and SW are not coupled in the longitudinal (x) direction. We therefore assume a constant atomic velocity in that direction, and simulate a longitudinal SW cross section by varying the strength of the optical potential with time during the interaction.

IV. BREAKDOWN OF THE RAMAN-NATH CONDITION

As a first demonstration of this simulation method, we show that the primary assumption of the Raman-Nath approximation, that the position wave function is unaltered by the interaction, breaks down well before the final momentum distribution predicted under that approximation becomes invalid. This result demonstrates the importance of atomic motion within a SW for interactions

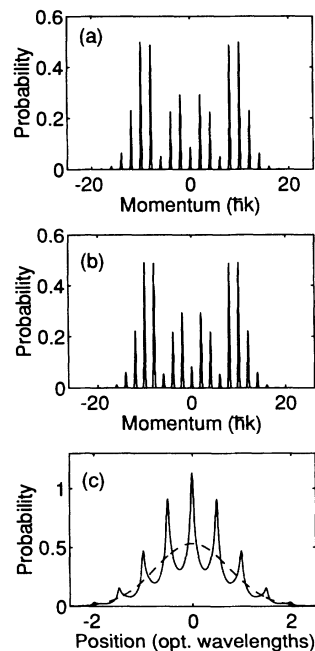


FIG. 2. (a) Momentum distribution from Raman-Nath calculation with $\Omega_0^2 t_{\text{int}}/\Delta = -12.0$. (b) Momentum distribution following interaction with the same parameters, but calculated using the method of Sec. III. (c) Dashed line: initial wave packet following the interaction, showing increased probability near the SW antinodes. Solid line: wave packet following the calculation in (b).

much shorter than one might assume from observation of the momentum distribution alone.

Calculation of the momentum distribution expected under the Raman-Nath approximation is straightforward. Since the atom is assumed to undergo no transverse motion, we can use the Schrödinger equation as in Eq. (2) but without the kinetic energy (second spatial derivative) term. The time-evolution operator for a SW interaction of duration t_{int} and with constant Ω_0 is thus

$$\begin{aligned}\hat{U}_{\text{RN}}(t_{\text{int}}) &= \exp\left(-\frac{i}{\hbar}V(y)t_{\text{int}}\right) \\ &= \exp\left(-i\frac{|\Omega_0|^2 t_{\text{int}}}{\Delta}\cos^2(ky)\right).\end{aligned}\quad (3)$$

Expanding $\hat{U}_{\text{RN}}(t_{\text{int}})$ in Bessel function form, the atom's momentum distribution following the interaction is given by

$$\begin{aligned}\langle p_y | \hat{U}_{\text{RN}}(t_{\text{int}}) | \phi \rangle &= \left\langle p_y \left| \exp\left(\frac{i|\Omega_0|^2 t_{\text{int}}}{2\Delta}\right) \left[J_0\left(\frac{|\Omega_0|^2 t_{\text{int}}}{2\Delta}\right) + 2 \sum_{n=1}^{\infty} i^n J_n\left(\frac{|\Omega_0|^2 t_{\text{int}}}{2\Delta}\right) \cos(2nky) \right] \right| \phi \right\rangle \\ &= \exp\left(\frac{i|\Omega_0|^2 t_{\text{int}}}{2\Delta}\right) \left[J_0\left(\frac{|\Omega_0|^2 t_{\text{int}}}{2\Delta}\right) \langle p_y | \phi \rangle \right. \\ &\quad \left. + \sum_{n=1}^{\infty} i^n J_n\left(\frac{|\Omega_0|^2 t_{\text{int}}}{2\Delta}\right) (\langle p_y + 2n\hbar k | \phi \rangle + \langle p_y - 2n\hbar k | \phi \rangle) \right],\end{aligned}\quad (4)$$

where the final form follows because of the cosine factor's action as a stepping operator in momentum space [11]. This result, for the parameters $\Omega_0^2 t_{\text{int}}/\Delta = -12.0$, appears in Fig. 2(a). (Units in this work are scaled in terms of recoil values. Here, the recoil frequency $\omega_{\text{rec}} = \hbar k^2/2m$ and the recoil time $t_{\text{rec}} = 2m/\hbar k^2$. Furthermore, we assume Ω_0 to be real.) As expected, the distribution is composed of a number of discrete scattering orders, separated by $2\hbar k$.

An interaction with the same parameters (specifically, $\Omega_0^2/\Delta = -485\omega_{\text{rec}}$ and $t_{\text{int}} = 0.025t_{\text{rec}}$), but calculated with the method of Sec. III yields the momentum distribution shown in Fig. 2(b). Although the momentum predictions from the two calculations are virtually indistinguishable, the position distribution obtained from the second shows significant distortion. The initial position wave packet appears as the dashed line in Fig. 2(c), while the wave packet immediately following the interaction is shown with the solid line. Note that the wave packet has begun to localize into peaks at intervals of half a standing wavelength as the dipole force attracts the atoms to the SW antinodes. Since the Raman-Nath approximation predicts no spatial deformation at all, it has clearly broken down even after a very short interaction.

This effect may have repercussions for recent proposals to determine the position of an atom in a SW via a measurement in which the phase shift of the optical field resulting from the interaction is monitored [12]. These schemes require that the field does not act back on the atom to alter its position wave function, and thus will be valid only for extremely brief interaction times.

V. LOCALIZATION IN THE NEAR FIELD

Following an interaction calculated using the method of Sec. III, it is possible to determine the wave packet's subsequent evolution through free space by applying the momentum space kinetic operator

$$\hat{U}_{\text{fs}}(t_{\text{fs}}) = \exp\left(-\frac{i}{\hbar}\frac{p_y^2}{2m}t_{\text{fs}}\right).\quad (5)$$

We find that the wave packet becomes strongly localized in position in the near field shortly after the interaction. As in the case of the localization within the SW described in the preceding section, the free-space focusing occurs at intervals of half an optical wavelength. Inside the SW, the wave packet was attracted to the antinodes. However, the momentum imparted to the wave packet in the SW provides a deflection such that after the interaction, the wave packet localizes behind the SW nodes. Figure 3 charts the free-space evolution of a wave packet whose

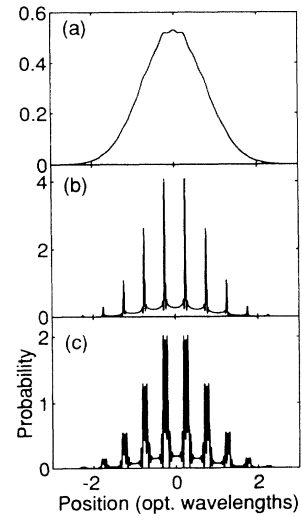


FIG. 3. Evolution of the wave packet in free space following the SW interaction shown in Fig. 2. (a) Disappearance of localization at SW antinodes after $t_{\text{int}} = 0.0125t_{\text{rec}}$. (b) Constructive interference of deflected wave packet components resulting in strong localization behind the SW nodes when $t_{\text{int}} = 0.035t_{\text{rec}}$. (c) At $t_{\text{int}} = 0.055t_{\text{rec}}$, the peaks are no longer as sharp, but contain more of the atomic probability.

position distribution upon leaving the SW is as in Fig. 2(c). At $t_{fs} = 0.0125t_{rec}$, shown in Fig. 3(a), the wave packet has smoothed out, nearly reconstructing its initial, preinteraction form. By $t_{fs} = 0.035t_{rec}$ [Fig. 3(b)], we observe localization into spikes with width $\approx 1/36$ of a standing wavelength. These spikes make up very little of the total atomic probability, which is contained mostly in the unlocalized baseline. However, by $t_{fs} = 0.055t_{rec}$ [Fig. 3(c)], the peaks have begun to spread out, and contain a much larger fraction of the probability.

Several groups have recently observed such near-field focusing by passing an atomic beam through a SW, which acts as an array of lenses, and depositing the focused atoms onto a substrate [13,14]. These authors explained their results using a semiclassical simulation of atomic trajectories in the dipole potential, but ignored effects due to the wave nature of the atoms.

VI. INTERACTION WITH A SECOND STANDING WAVE

Once the wave packet has become well localized in the near field following the interaction and free propagation described above (but this time with $t_{fs} = 0.048t_{rec}$), we may arrange for it to interact with a second SW. If the potential of the second SW is offset from that of the first by an eighth of a wavelength in the y direction, the peaks in the wave packet will pass through regions with a high potential gradient [see Fig. 4(a)]. The second SW, for which $\Omega_0^2/\Delta = 18060\omega_{rec}$ and $t_{int} = 0.0061t_{rec}$

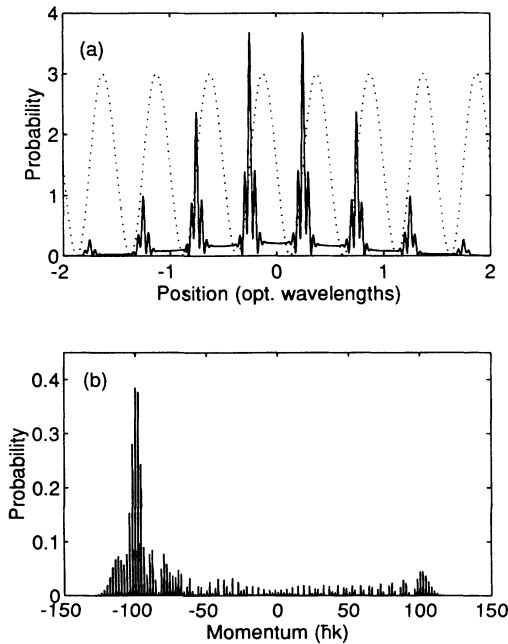


FIG. 4. Deflection of an atomic wave packet by interaction with two SW's. (a) Solid line: wave packet at time $t_{fs} = 0.048t_{rec}$ after the first interaction. Dotted line: location of the potential of the second SW with respect to the wave packet. (b) Atomic momentum distribution following the second interaction, showing strong deflection.

(i.e., $\Omega_0^2 t_{int}/\Delta = 110.8$), thus exerts an asymmetrical transverse force on the atom, whose resulting momentum distribution after the second interaction appears in Fig. 4(b). From this figure, it is clear that the SW has efficiently deflected the atomic momentum by $\approx 100\hbar k$.

For ${}^4\text{He}$ interacting with a laser tuned near the 2^3S_1 - 2^3P_2 transition at $1.083\ \mu\text{m}$, the velocity corresponding to a transverse momentum of $100\hbar k$ is $9\ \text{ms}^{-1}$. Since a typical (supersonic) beam of He atoms has a longitudinal velocity of $1760\ \text{ms}^{-1}$ [2], the deflection angle for the mirror described above is thus 5 mrad. Such a deflection compares favorably with that reported for atomic reflection from an evanescent wave mirror [15].

Next, consider a situation that begins with an initial SW interaction identical to that in the previous case. This time, however, the wave packet interacts with a second SW whose period is twice that of the first and for which $\Omega_0^2/\Delta = 72250\omega_{rec}$ and $t_{int} = 0.0061t_{rec}$ (i.e., $\Omega_0^2 t_{int}/\Delta = 443.4$). Now, successive peaks of the wave packet pass through regions of alternating potential gradient [see Fig. 5(a)], which exert equal but opposite forces on different parts of the wave packet. As a result, the atomic momentum distribution is split into two widely separated peaks, as shown in Fig. 5(b). This setup therefore acts as an efficient atomic beam splitter. As such, it produces output similar to that of the magneto-optical beam splitter [3], which uses a magnetic field parallel to a single SW to split an atomic beam into two narrow outputs separated by $\approx 40\hbar k$.

The relative amounts of momentum acquired by the

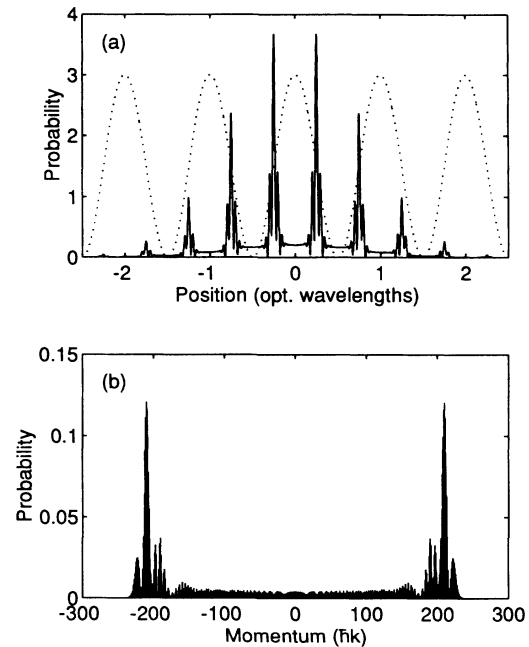


FIG. 5. Splitting of an atomic wave packet by interaction with two SW's. (a) Solid line: wave packet at time $t_{int} = 0.048t_{rec}$ after the first interaction. Dotted line: location of the potential of the second SW with respect to the wave packet. Note that the period of the second SW is twice that of the first. (b) Atomic momentum distribution following the second interaction, showing symmetrical bifurcation.

atoms in the two examples above are straightforward to explain. The depth of the optical potential of the SW shown in Fig. 5(a) is four times that of the SW shown in Fig. 4(a). However, since the period of the SW of Fig. 5(a) is twice that of the SW in Fig. 4(a), the gradient of the optical potential (and hence the dipole force) in the second example is double that of the first.

Note that in the absence of spontaneous emission, these deflection processes are coherent. Therefore the output beams can be used for interferometric phase measurements.

An experimental observation of these deflections would require careful positioning and control of the SW's relative to each other and to the atomic beam. In particular, the proper spatial phase relationship between the two SW's is critical, and must be kept constant for the duration of a measurement. Furthermore, the separation between the SW's should be maintained quite carefully; for the ^4He case above, this separation is $320 \mu\text{m}$. Such a separation, while not much greater than the required widths of the SW's, should be experimentally feasible.

VII. SHIFTED-POTENTIAL BEAM SPLITTER

We now describe a particular single SW interaction that can act directly as a beam splitter as follows. First, a pulse of atoms incident on a positive detuned SW is allowed to become localized at the low-potential regions (field nodes.) Then, the spatial phase of the SW is shifted by a quarter wavelength in a time short enough that the atomic motion during the shift is minimal. After the shift, the atoms find themselves at the high-potential antinodes. Once again, they will be attracted to the nodes, and thus acquire positive or negative transverse momentum depending toward which adjacent node they move.

In practice, the splitting process is slightly more subtle than the simple scheme described above, particularly when effects due to a time-dependent SW cross section are taken into account. We will follow an example interaction in detail to illustrate its basic mechanism. Consider a wave packet with a transverse position spread of 1.2 optical wavelengths incident on a SW with a Gaussian longitudinal cross section and a potential depth whose mean value is $\Omega_0^2/\Delta = 1210\omega_{\text{rec}}$. The duration of the interaction is $t_{\text{int}} = 0.195t_{\text{rec}}$. The dipole force attracts the initial wave packet, shown as the dashed line in Fig. 6(a), to the SW nodes, at which the wave packet becomes localized after $t = (4/15)t_{\text{int}}$, as the solid line in Fig. 6(a) shows. Its momentum distribution at this time appears in Fig. 7(a). This localization is only transient, however, and by $t = (2/5)t_{\text{int}}$ the wave packet has spread to cover most of the regions of low potential [see Fig. 6(b)]. Its momentum distribution subsequently narrows, as shown in Fig. 7(b). At this time, t_{shift} , we shift the phase of the SW by $\lambda/4$, so that the wave packet, which was mostly in regions of low potential, finds itself concentrated on potential hills. This phase shift cannot take place instantaneously in order to avoid violating adiabatic conditions; here the shift duration is $t_{\text{shift}}/300$. As

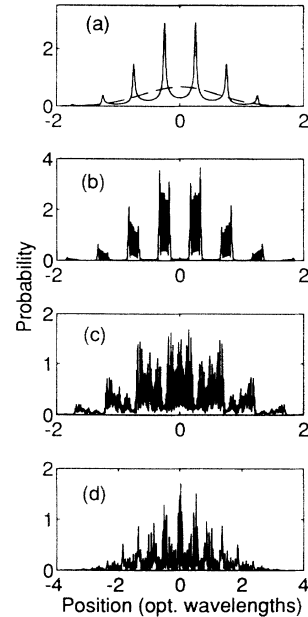


FIG. 6. Evolution of position distribution of an atomic wave packet during a shifted-potential interaction. See text for a description of each subfigure.

the SW shifts, it exerts an extra transverse force on the wave packet, which results in the slightly asymmetrical profiles in Figs. 6–8.

The structure in the position distributions on a scale much smaller than a standing wavelength is the result of interference between various components with different momenta.

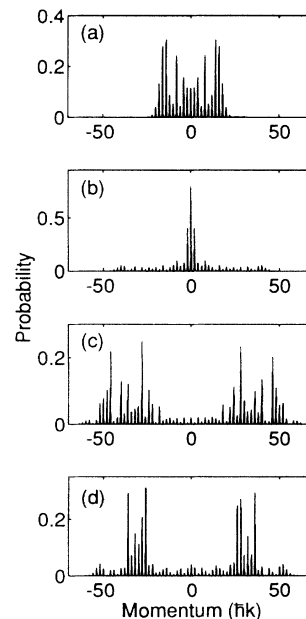


FIG. 7. Evolution of momentum distribution of an atomic wave packet during a shifted-potential interaction. See text for a description of each subfigure.

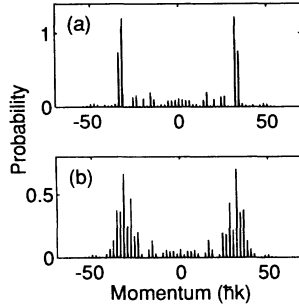


FIG. 8. Final momentum distributions for shifted-potential interactions with the parameters (a) $\Omega_0^2/\Delta = 1008\omega_{\text{rec}}$, $t_{\text{int}} = 0.314t_{\text{rec}}$, $t_{\text{shift}} = (2/5)t_{\text{int}}$; (b) $\Omega_0^2/\Delta = 1008\omega_{\text{rec}}$, $t_{\text{int}} = 0.262t_{\text{rec}}$, $t_{\text{shift}} = (2/5)t_{\text{int}}$.

At and shortly after the time of the shift, the wave packet is in the most intense part of the SW. It is thus attracted strongly to the new nodes. The wave packet can be seen moving away from the new potential hills toward the new nodes in Fig. 6(c), and its momentum distribution, in Fig. 7(c), has clearly split. The fastest momentum components in the wave packet have enough time and energy to pass through the new nodes and be slowed slightly by moving up the adjacent potential hills. Since the intensity of the SW drops off quite quickly at this point, the slower components are scarcely reflected by these potential hills, and can thus “catch up” with the faster parts. As a result, the final momentum distribution after the interaction, shown in Fig. 7(d), consists of two fairly narrow but widely spaced clusters of diffraction orders, which together contain over two-thirds of the probability. Thus most of the atoms in the pulse will end up in one of these two output beams in the far field. Figure 6(d) shows the final position distribution, which spreads out as the confining optical potentials decrease.

Two other final momentum distributions, for the parameters shown, appear in Fig. 8 to give some idea of the range of possible results. Specifically, it is possible to produce fairly broad output beams that contain virtually all of the atomic probability, or very narrow ones containing a somewhat smaller fraction of the total number of atoms, by varying the interaction parameters slightly.

Since this technique is quite sensitive to the time at which the phase of the SW shifts, it is limited to very short pulses. Alternatively, it could be applied to a small cloud of cooled atoms that had just been released from a magneto-optical trap. In that case, a SW of large enough diameter that the entire atomic cloud was within a region of nearly constant longitudinal cross section could be turned on around the cloud. The SW intensity could be given a Gaussian variation in time, and its phase could be shifted at the appropriate time. Then, the two groups of atoms that had received opposite transverse momenta would separate as they fell under gravity.

For Cs in a SW tuned near its D_2 line at 852 nm, the required duration of the interaction in Figs. 6 and 7 is $t_{\text{int}} = 1.5 \times 10^{-5}$ s. Since the natural lifetime of the Cs D_2 transition is 3×10^{-8} s, a large detuning from resonance will be necessary to suppress spontaneous emis-

sions. We estimate that a detuning $\Delta \approx 5$ GHz, and a Rabi frequency $\Omega_0 \approx 110$ MHz will provide the necessary ac Stark potential while keeping the probability of spontaneous emission to less than 25%. Producing that Rabi frequency for that detuning in a Cs D_2 transition requires a laser intensity of about 250 W m^{-2} , which over a SW of radius 5 mm corresponds to a laser power of about 20 mW.

VIII. ATOMIC MOMENTUM COMPRESSION BY A STANDING WAVE

Finally, we show that the transverse-momentum distribution of an atomic beam passing through an antinode of a negative detuned SW can be significantly compressed. Consider an interaction for which $\Omega_0^2/\Delta = -1000\omega_{\text{rec}}$ and $t_{\text{int}} = 0.025t_{\text{rec}}$, and for which the SW has a Gaussian longitudinal cross section. The wave packet, whose initial position and momentum distributions are shown as the dashed lines in Fig. 9, at first can spread out to cover the low potential area around the antinode. However, as it moves up into regions of higher potential, it loses kinetic energy, and its momentum spread subsequently narrows. We choose the interaction duration such that the SW intensity has begun to drop off quickly at this point; as a result, the wave packet does not reflect from the regions of high potential and thus regain its transverse momentum.

The final position and momentum distributions appear as the solid lines in Fig. 9. Because the momentum profile has narrowed, the rate of transverse spreading of the atomic beam is greatly reduced; that is, the beam has become well collimated. As a result, this interaction acts as the atom optical analog of a beam expander.

The initial wave function is a minimum position-momentum uncertainty state, for which $\Delta p_y \Delta y = \hbar/2$. This uncertainty relation changes very little during the interaction; the final state is such that $\Delta p_y \Delta y = 0.54\hbar$.

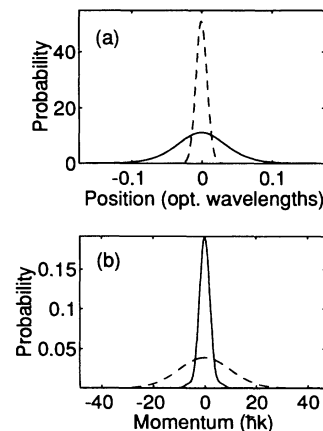


FIG. 9. (a) Initial (dashed) and final (solid) position distributions for a wave packet passing through a negative detuned SW antinode. (b) Initial (dashed) and final (solid) momentum distributions for the same interaction, showing significant reduction in width.

IX. CONCLUSION

We have outlined a numerical method for calculating the position and momentum distributions of an atomic wave packet as it passes through a laser standing wave. With this method, we have shown that the Raman-Nath criterion breaks down for shorter interaction times than one might infer from study of the final momentum distribution alone. We have proposed a method for deflecting or splitting a continuous atomic beam based on two SW interactions applied in quick succession. Furthermore, we describe a technique for splitting a pulsed atomic beam with a single SW by quickly shifting the SW phase part-way through the interaction. The coherence and high effi-

ciency possible with these schemes should make them attractive candidates in atom interferometers that require a large separation between the two paths. Finally we describe an atom optical beam expander in which the transverse-momentum spread of an atomic beam can be compressed by passage through a SW antinode.

ACKNOWLEDGMENTS

This work is financially supported by the Rhodes Trust, the Royal Society, and the U.K. Science and Engineering Research Council.

-
- [1] P. L. Gould, P. J. Martin, G. A. Ruff, R. E. Stoner, J.-L. Picque, and D. E. Pritchard, *Phys. Rev. A* **43**, 585 (1991).
 - [2] T. Sleator, T. Pfau, V. Balykin, and J. Mlynek, *Appl. Phys. B* **54**, 375 (1992).
 - [3] T. Pfau, Ch. Kurtsiefer, C. S. Adams, M. Sigel, and J. Mlynek, *Phys. Rev. Lett.* **71**, 3427 (1993).
 - [4] C. S. Adams, M. Sigel, and J. Mlynek, *Phys. Rep.* (to be published).
 - [5] E. Schumacher, M. Wilkens, P. Meystre, and S. Glasgow, *Appl. Phys. B* **54**, 451 (1992).
 - [6] J. Chen, J. G. Story, and R. G. Hulet, *Phys. Rev. A* **47**, 2128 (1993).
 - [7] U. Janicke, C. S. Adams, and M. Wilkens (unpublished).
 - [8] J. Dalibard and C. Cohen-Tannoudji, *J. Opt. Soc. Am. B* **2**, 1707 (1985).
 - [9] A. P. Kazantsev, G. I. Surdutovich, and V. P. Yakovlev, *Mechanical Action of Light on Atoms* (World Scientific Press, Singapore, 1990).
 - [10] W. H. Press, B. P. Flannery, S. A. Teukolsky, and W. T. Vetterling, *Numerical Recipes in C* (Cambridge University Press, Cambridge, England, 1988).
 - [11] M. Lindberg, *Appl. Phys. B* **54**, 467 (1992).
 - [12] P. Storey, M. Collett, and D. Walls, *Phys. Rev. Lett.* **68**, 472 (1992); M. A. M. Marte and P. Zoller, *Appl. Phys. B* **54**, 477 (1992).
 - [13] G. Timp, R. E. Behringer, D. M. Tennant, J. E. Cunningham, M. Prentiss, and K. K. Berggren, *Phys. Rev. Lett.* **69**, 1636 (1992).
 - [14] J. J. McClelland, R. E. Sholten, E. C. Alm, and R. J. Celotta, *Science* **262**, 877 (1993).
 - [15] V. I. Balykin, V. S. Letokhov, Yu. B. Ovchinnikov, and A. I. Sidorov, *Phys. Rev. Lett.* **60**, 2137 (1988); J. V. Hajnal, K. G. H. Baldwin, P. T. H. Fisk, H.-A. Bachor, and G. I. Opat, *Opt. Commun.* **73**, 331 (1989); W. Seifert, C. S. Adams, V. I. Balykin, C. Heine, Yu. Ovchinnikov, and J. Mlynek, *Phys. Rev. A* **49**, 3814 (1994).